

Electronic Supplementary Information

From 3D channelled frameworks to 2D layered structures in molecular salts of L-serine and DL-serine with oxalic acid

Dario Braga, Laura Chelazzi, Iacopo Ciabatti and Fabrizia Grepioni

Università di Bologna, Dipartimento di Chimica G. Ciamician, Via Selmi 2, 40126 Bologna

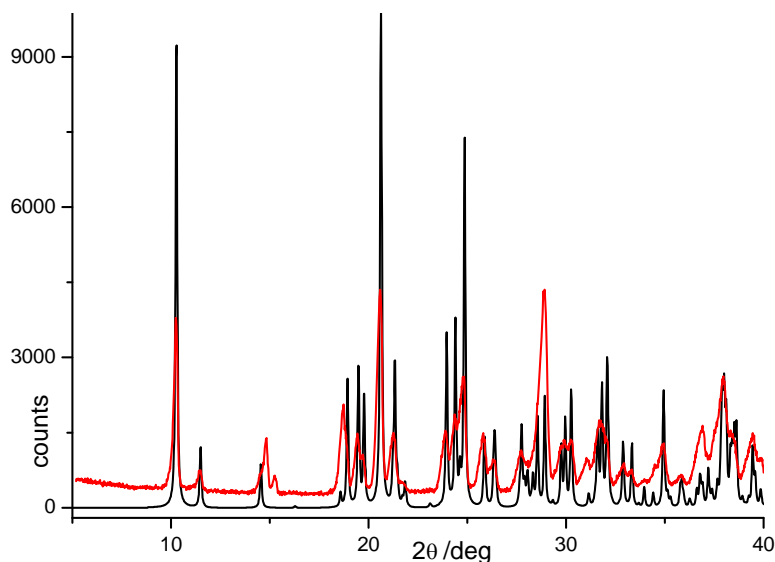


Figure ESI-1. Comparison of X-ray powder patterns for crystalline [DL-serH]₂[ox]·2H₂O, calculated on the basis of single crystal data (black line) and measured (red line) on the product of kneading of DL-serine and oxalic acid in 1:1 ratio. Residual peaks of oxalic acid are present in the experimental pattern.

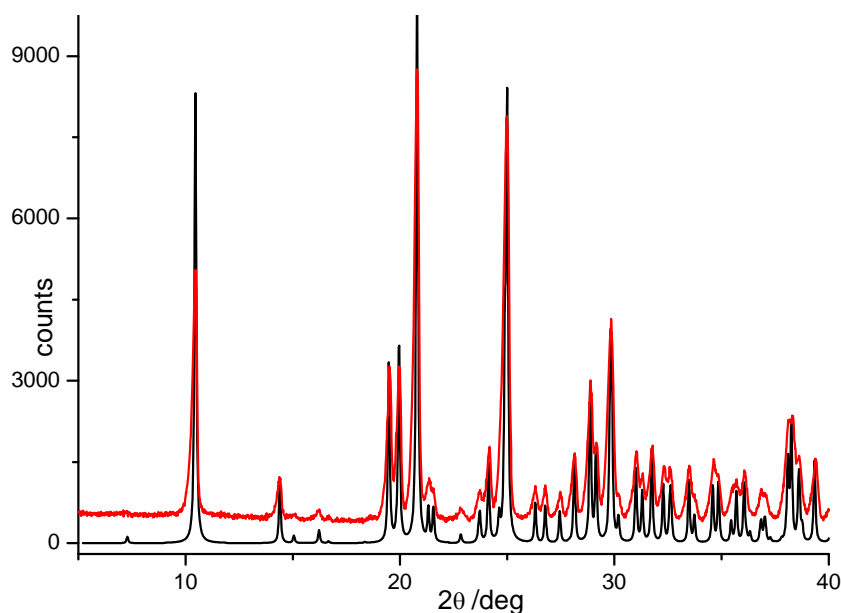


Figure ESI-2. Comparison of X-ray powder patterns for crystalline [L-serH]₂[ox]·2H₂O form I, calculated on the basis of single crystal data (black line) and measured (red line) on the product of kneading of L-serine and oxalic acid in 2:1 ratio.

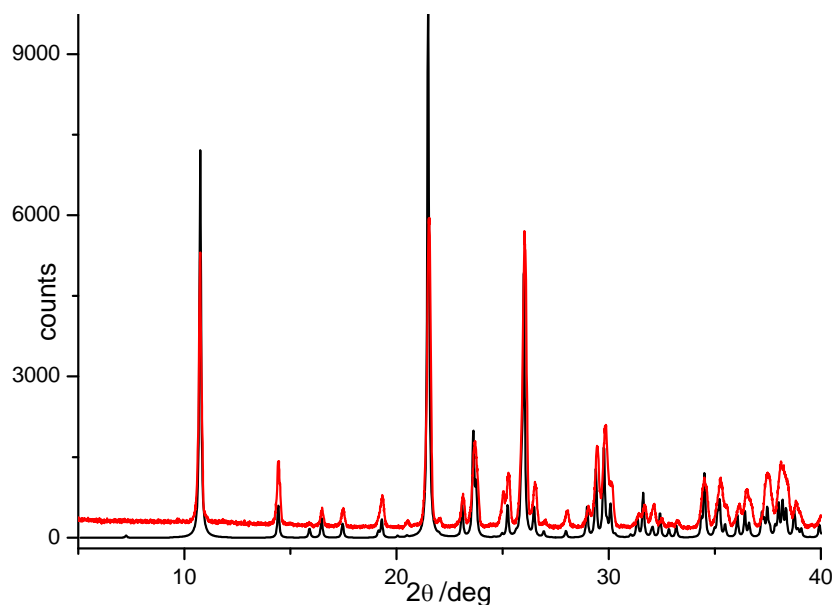


Figure ESI-3. Comparison of X-ray powder patterns for crystalline $[\text{L-serH}]_2[\text{ox}] \cdot 2\text{H}_2\text{O}$ form II, calculated on the basis of single crystal data (black line) and measured (red line) on the product of grinding of L-serine and oxalic acid in 2:1 ratio.

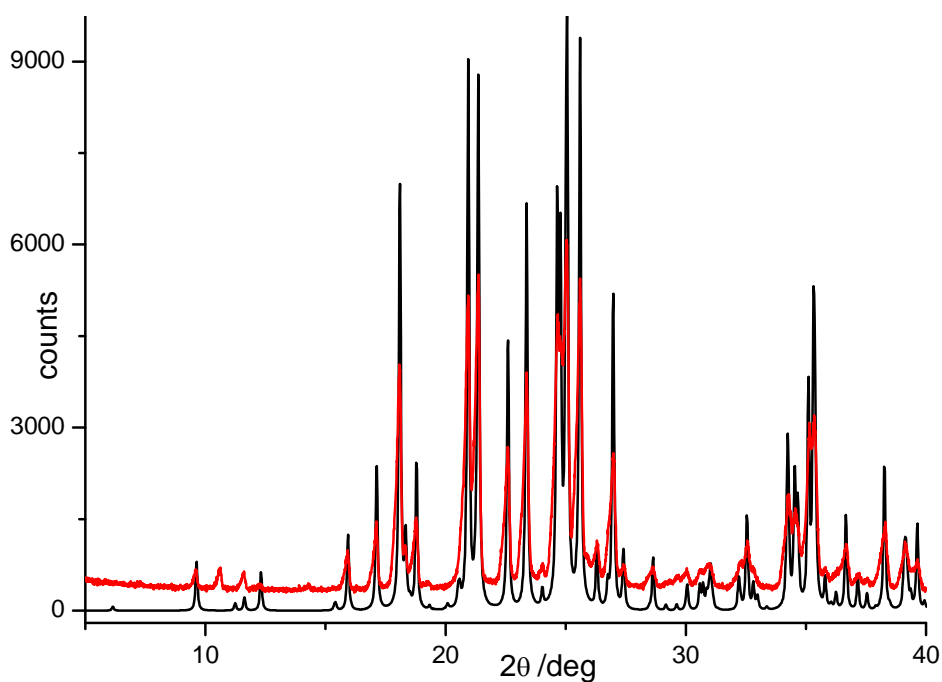


Figure ESI-4. Comparison of X-ray powder patterns for crystalline $[\text{L-serH}][\text{Hox}]$, calculated on the basis of single crystal data (black line) and measured (red line) on the product of grinding of L-serine and oxalic acid in 1:1 ratio.

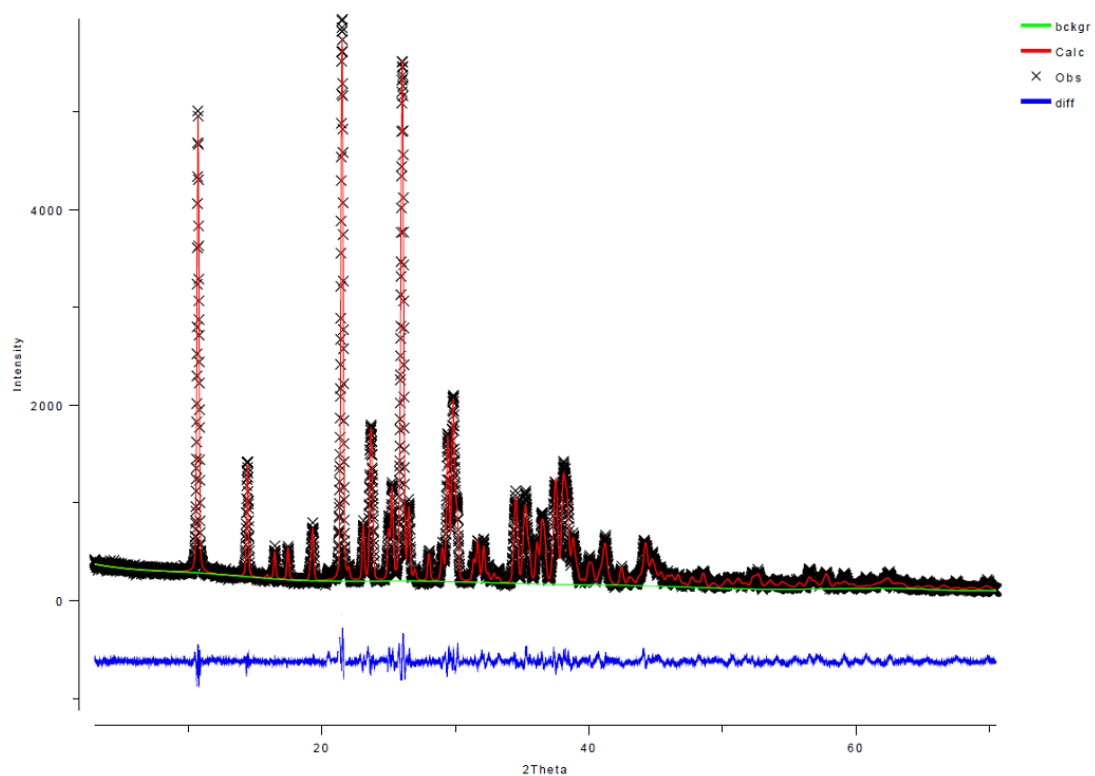


Figure ESI-5. Final Rietveld refinement plot for [L-serH]₂[ox]·2H₂O Form II

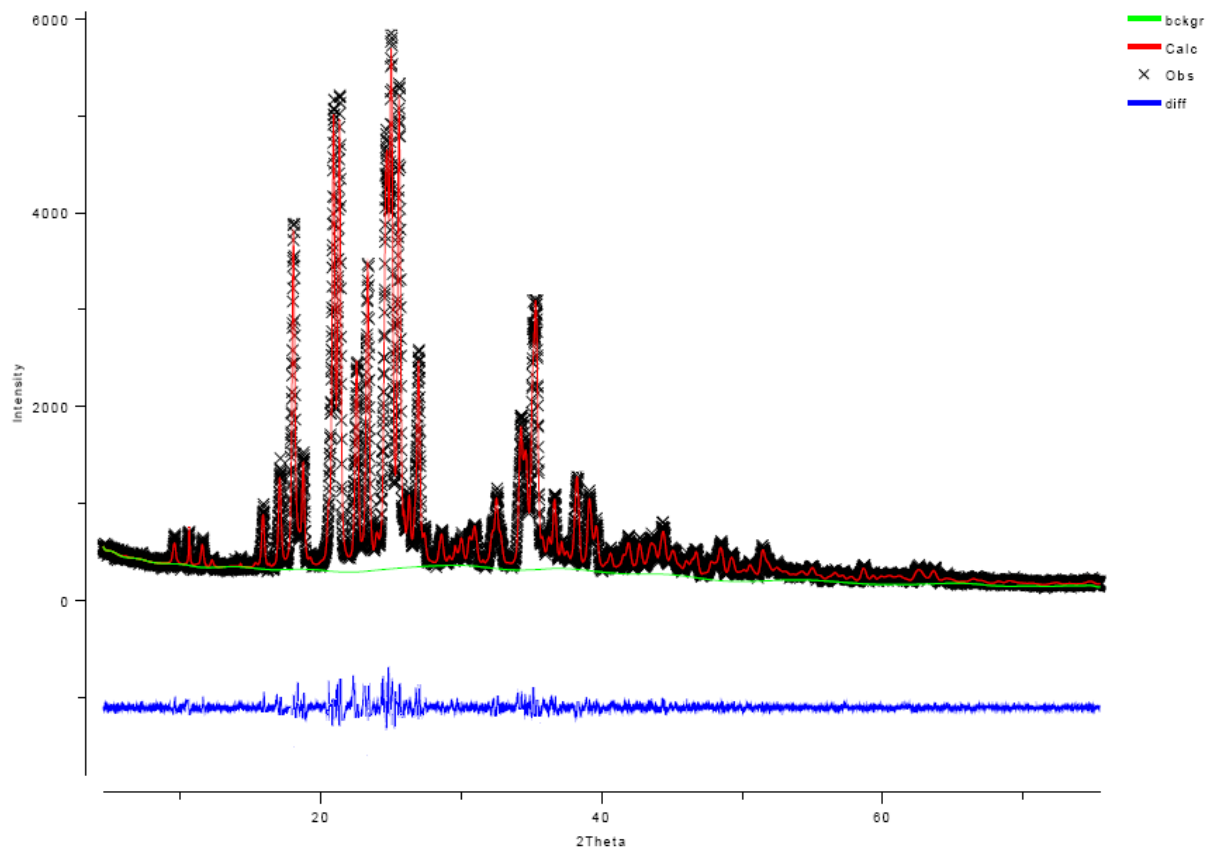


Figure ESI-6. Final Rietveld refinement plot for anhydrous [L-serH][Hox]

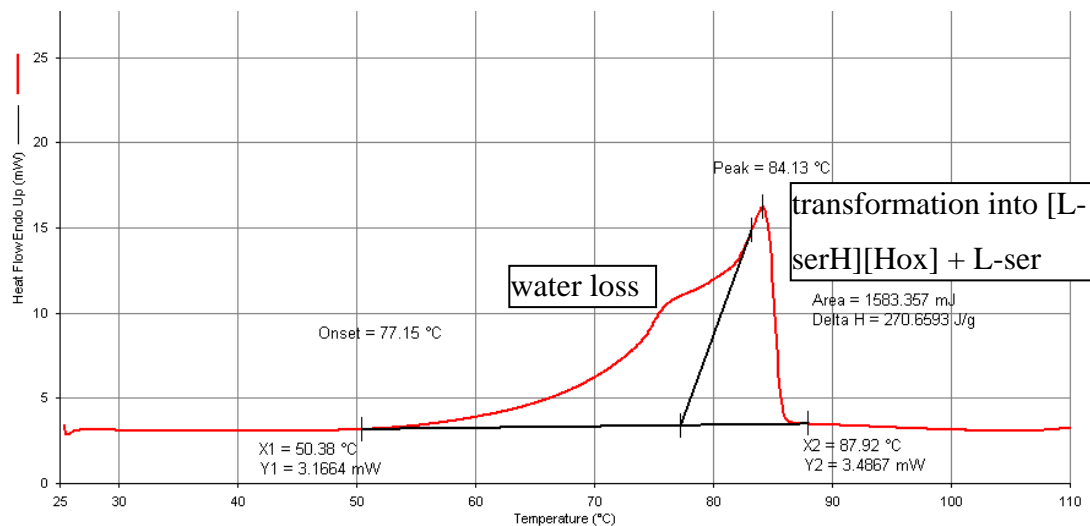


Figure ESI-7. DSC in open pan of [L-serH]₂[ox]·2H₂O form I : loss of water followed by transformation into [L-ser][Hox] + L-ser.

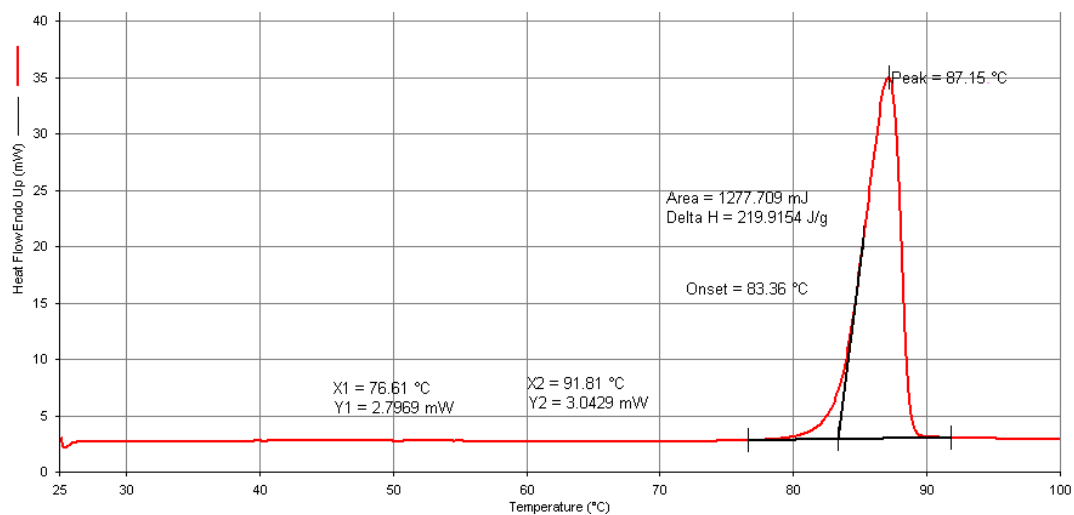


Figure ESI-8. DSC in sealed pan of [L-serH]₂[ox]·2H₂O form I (congruent melting).

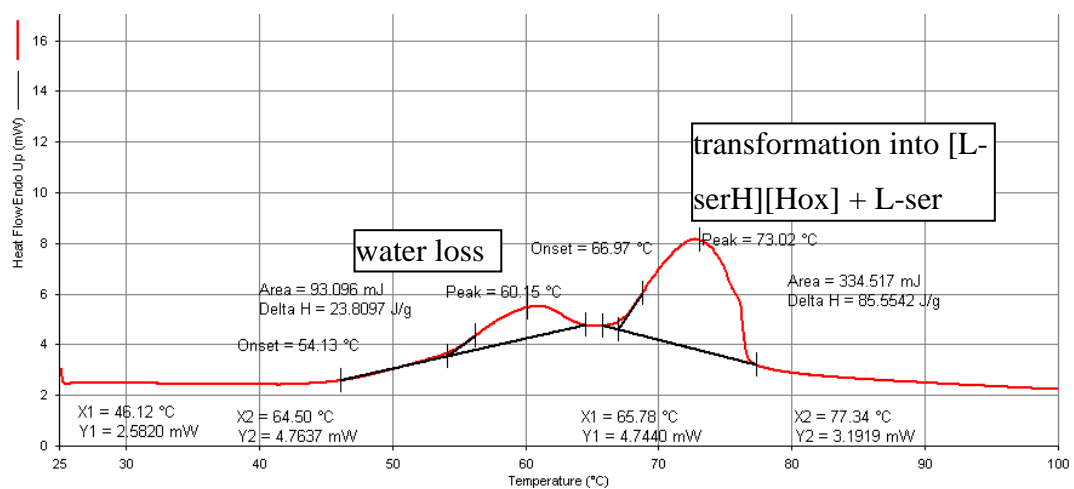


Figure ESI-9. DSC in open pan of [L-serH]₂[ox]·2H₂O form II: loss of water followed by transformation into [L-ser][Hox] + L-ser.

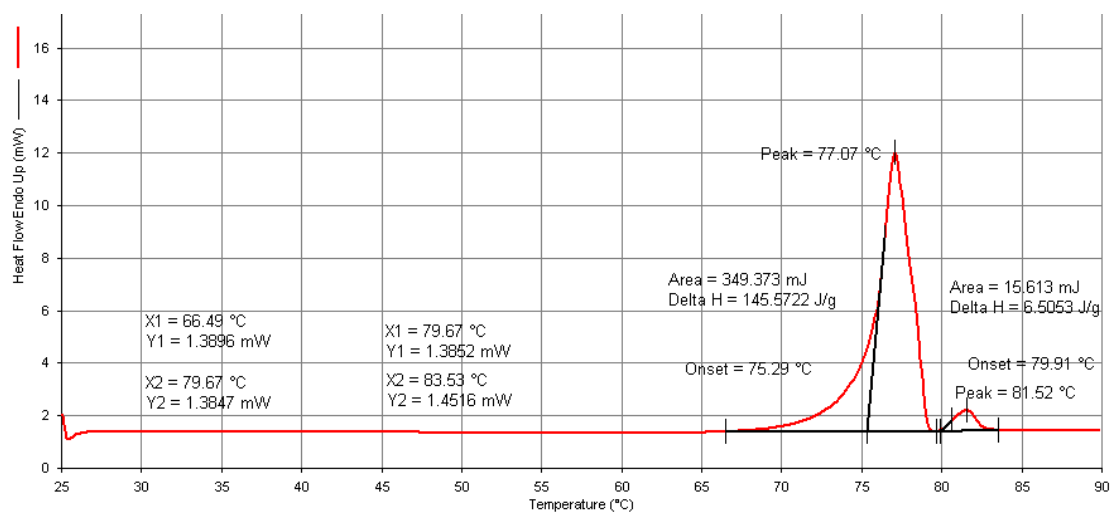


Figure ESI-10. DSC in sealed pan of [L-serH]₂[ox]·2H₂O form II.

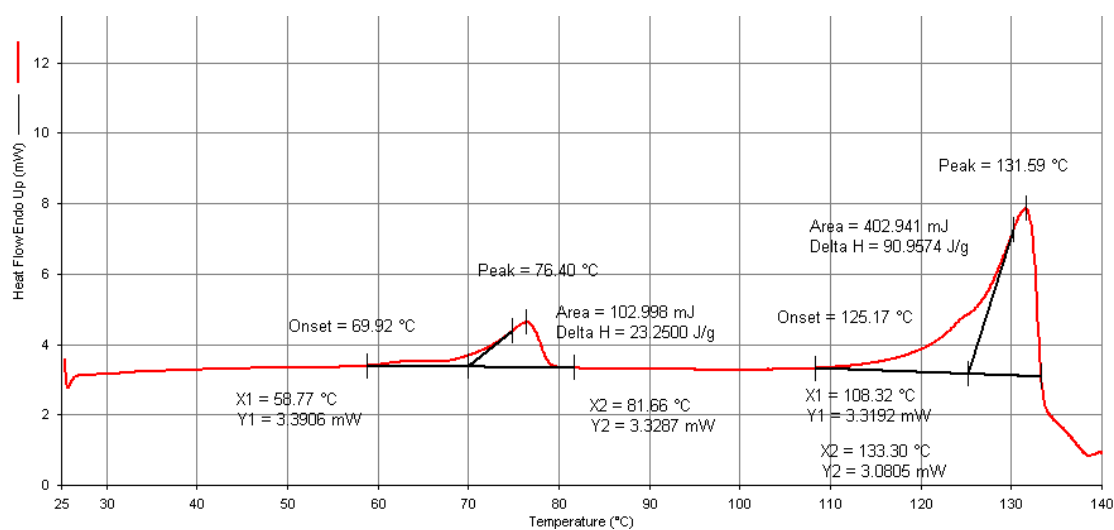


Figure ESI-11. DSC in open pan of [L-serH][Hox]: the first peak is due to an impurity of Form II.

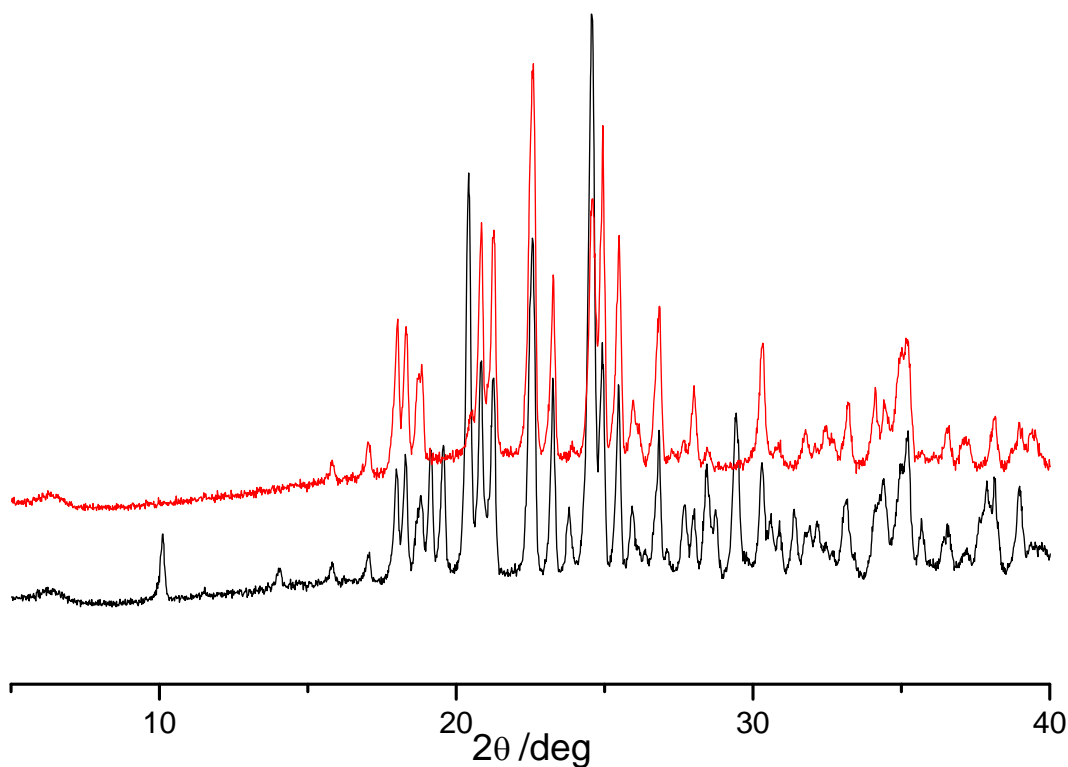


Figure ESI-12. Variable temperature X-ray powder diffraction measurements for [L-serH]₂[ox]·2H₂O form I: at 80°C (black line) partial transformation into [L-serH][Hox] plus L-ser is observed, which is complete at 85°C (red line).

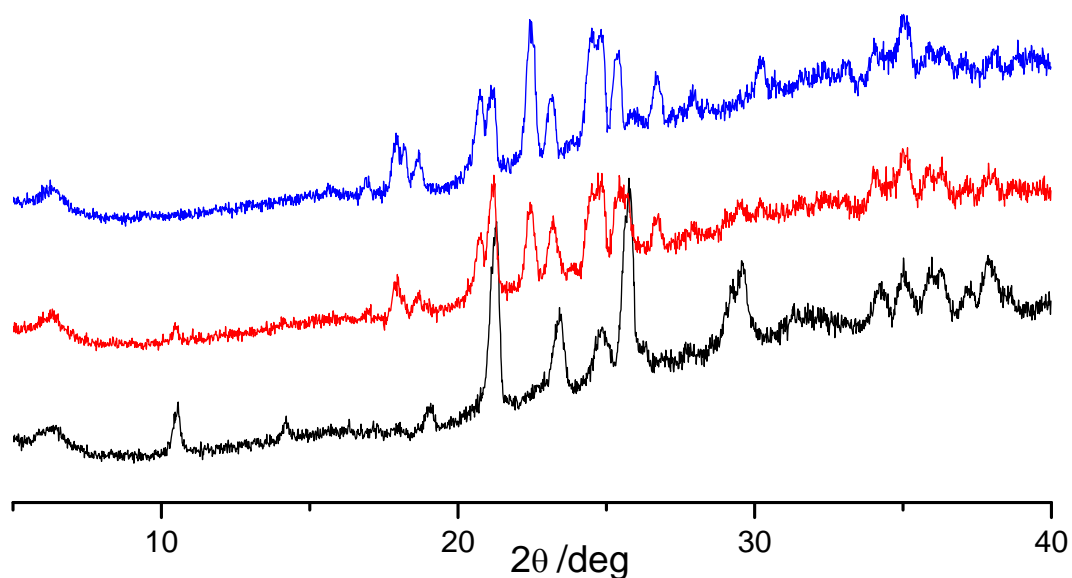


Figure ESI-13. Variable temperature X-ray powder diffraction measurements for [L-serH]₂[ox]·2H₂O form II (black line at RT): at 70°C (red line) partial transformation into [L-serH][Hox] plus L-ser is observed, which is complete at 75°C (blue line).